

DESIGN ON TRACTION BRAKING CHARACTERISTICS TEST OF TRACTION MOTOR FOR RAIL TRANSIT

Yongchao Xie,* Jun Yan,** Li Yang,* Hui Zhang,*** and Canhui Wu****

Abstract

Traction braking characteristics are an important parameter index to measure the performance of rail transit traction motors. Using the general mathematical model of rail transit traction motor, the traction braking characteristics of rail transit traction motor are analysed in detail, and the control strategy of rail transit traction motor operation and the typical characteristic parameters of rail transit traction motor are deduced. According to the operation control strategy of the rail transit traction motor, the rail transit traction motor intelligent integrated test system produced by Hunan Xinen Intelligent Technology Co., Ltd. is used in the traction system of the 200 kW Bombardier MJC250-7 rail transit traction motor used in Lanzhou Rail Transit Co., Ltd. The dynamic characteristics were tested, and the traction braking characteristic test parameters and performance test curves were obtained. It provides reference for testing traction and braking parameters of rail transit traction motors.

Key Words

Rail transit traction motor, traction braking characteristics, test

1. Introduction

In recent years, China's urban rail transit has developed rapidly. Urban rail transit has played an extremely important role in meeting the travel needs of the people and supporting and leading urban development. As of the end of September 2019, the total mileage of urban rail transit operations in China has exceeded 6,300 km [1]. The carrying capacity and traction performance of urban rail transit vehicles mainly depend on the torque and speed characteristics of rail transit traction motors. The

AC traction motors used in urban rail transit have no commutation restrictions. Therefore, the rail transit traction motor can be started with a relatively large constant torque. At the same time, its constant power speed regulation range is relatively wide. In addition, it can withstand the transient process and has a wide range of smooth speed regulation, so that the process of traction, braking, and speed regulation of urban rail transit vehicles is fast. Moreover, the adhesion performance and dynamic control performance of the AC traction motor used in urban rail transit are superior, so that it has a higher power-to-volume ratio and cost-effectiveness [2], [3].

At present, the research status of the traction braking characteristics of urban rail transit traction motors is as follows: Zhuzhou Converter Technology National Engineering Research Center Co., Ltd. He *et al.* [3] proposed a new type of traction braking characteristic for the AC traction motor (MTA A4-200, 190 kW) produced by Ansaldo Breda for urban rail transit. Test method, they theoretically analysed the influence of traction braking characteristics on the performance of traction motors; Tao *et al.* [4] from Lanzhou Jiaotong University used MATLAB/Simulink simulation software to simulate the traction performance of a 190 kW subway traction motor; Wang [5] proposed an optimisation plan for the characteristics of the braking system of Nanjing Metro Line 3 vehicles; Gong [6] of Shenzhen University has constructed a theoretical model of urban rail transit vehicle motion equation and energy consumption calculation for the three states of urban rail transit vehicle traction, idling, and braking; Li *et al.* [7] conducted design and performance calculation simulations for the traction and electric braking characteristics of urban rail transit vehicles on Chongqing Metro Line 6; Huang *et al.* [8] used binary search and Lagrangian interpolation algorithm to derive the calculation method of urban rail transit locomotive traction/braking envelope. The existing research on the traction and braking characteristics of urban rail transit traction motors is biased towards the theoretical analysis, modelling, derivation, and simulation analysis of the traction braking characteristics of traction motors [9]–[16]. Such as, Sudeshna *et al.* [17] proposed an adaptive motor control algorithm based on genetic algorithm (GA)

* Hunan Railway Professional Technology College, Zhuzhou 412001, Hunan, China; e-mail: xieyongchao2008@126.co; 413656787@qq.com

** Central South University, Changsha 410083, China; e-mail: 923432562@qq.com

*** Lanzhou Rail Transit Co. Ltd., Lanzhou 730030, China; e-mail: 695545088@qq.com

**** Hunan Xinen Intelligent Technology Co., Ltd., Zhuzhou 412001, Hunan, China; e-mail: wucanhui@126.com

Corresponding author: Li Yang

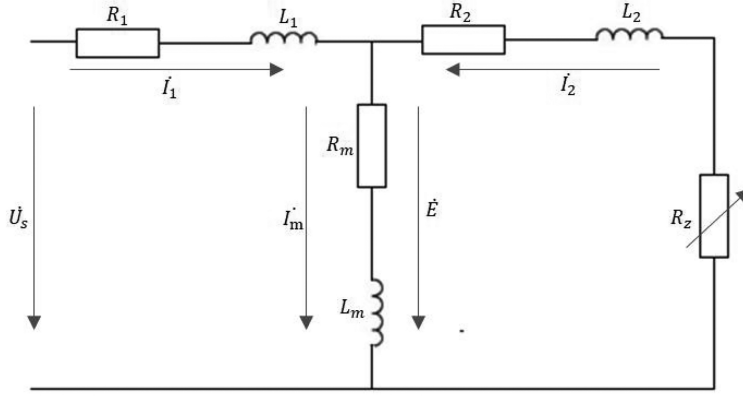


Figure 1. Mathematical model diagram of rail transit traction motor calculation.

and artificial bee colony (ABC). Shirish Murty *et al.* [18] proposed a new brushless DC switched reluctance motor structure for modern railway locomotives, which can provide higher speed and reliable operation on the existing guideway system. Shi *et al.* [19] discusses the relationship between the gear fault characteristics and the electrical harmonic frequency components in the stator current signals of the asynchronous motor inverter. The carbon-fibre-wrapped synchronous reluctance traction motor is tested [20]. Paul *et al.* [21] studied the traction characteristics of traction motors for high-speed trains in Korea. Traction motor speed was tested on Indian Railways locomotive [22]. But, there is a lack of actual testing of the relevant parameters and performance curves of the traction braking characteristics of rail transit traction motors.

This article is aimed at the actual needs of the traction braking characteristic test of the rail transit traction motor. The general mathematical model of rail transit traction motors is used and detailed theoretical analysis and derivation are carried out. The rail transit traction motor intelligent comprehensive test system produced by Hunan Xinen Intelligent Technology Co., Ltd. was used to test and verify the traction braking characteristics of the 200 kW Bombardier MJC250-7 rail transit traction motor used in Lanzhou Rail Transit Co., Ltd. This article contains analysis of theoretical model of traction motor for rail transit, analysis of traction characteristics of traction motors in rail transit, analysis of braking characteristics of traction motors in rail transit, and traction braking characteristic test of rail transit traction motor and conclusions.

2. Analysis of Theoretical Model of Traction Motor for Rail Transit

The traction motors used in urban rail transit usually use AC asynchronous motors, and its calculation mathematical model can be shown in Fig. 1.

L_1 is the stator reactance of the traction motor, R_1 is the stator resistance of the traction motor; L_2 is the equivalent leakage reactance of the traction motor rotor, R_2 is the equivalent resistance corresponding to the copper loss of the traction motor rotor; L_m is the excitation reactance of the traction motor, R_m is the excitation

resistance of the traction motor; R_z is the equivalent resistance corresponding to the mechanical power of the rotor shaft of the traction motor; \dot{I}_1 is the stator current of the traction motor; \dot{I}_2 is the equivalent current of the traction motor rotor; \dot{I}_m is the excitation current of the traction motor; \dot{E} is the induced potential of the main magnetic flux of the traction motor; and \dot{U}_s is the power supply voltage for the traction motor [3].

R_z can be expressed by (1), and S is the slip rate of the rail transit traction motor [9].

$$R_z = \frac{1-S}{S} R_2 \quad (1)$$

According to the mathematical model of rail transit traction motor calculation and KVL/KCL equation in Fig. 1, the basic expression of rail transit traction motor can be derived, as shown in (2), and \dot{E}_2 is the equivalent value of the rotor potential of the traction motor.

$$\begin{cases} \dot{U}_s = \dot{I}_1 (R_1 + jL_1) + \dot{I}_m (R_m + jL_m) \\ \dot{I}_m = \dot{I}_1 + \dot{I}_2 \\ \dot{E}_2 = \dot{I}_2 [(R_2 + jL_2) + R_z] \end{cases} \quad (2)$$

When the rail transit traction motor is operating in traction conditions, the slip ratio can be derived according to the (2) and the mathematical model diagram of the rail transit traction motor calculation in Fig. 1. [9], as shown in (3):

$$S = \frac{R_2 \dot{I}_2}{\dot{E}_2 \cos \varphi} \quad (3)$$

It can be seen from (3) that when the rail transit traction motor is in the traction mode, if its load increases, \dot{I}_2 will inevitably increase, which will also lead to an increase in S , and n_1 is decreased.

If the rail transit traction motor is in the braking condition, its speed (n_1) will be greater than the synchronous speed (n). At this time, the slip rate (S) of the traction motor is less than 0, and the rotor loop resistance of the traction motor is also less than 0. According to (2) and Fig. 1, the calculation methods of the total mechanical power (P_J) and electromagnetic power (P_{em}) of the rotor side of the traction motor can be derived, as shown in (4)

and (5):

$$P_J = m_2 \left(\dot{I}_2 \right)^2 R_z \quad (4)$$

$$P_{em} = m_2 \left(\dot{I}_2 \right)^2 (R_z + R_2) \quad (5)$$

According to (2) and Fig. 1, it can be derived that the full mechanical power of the rotor side of the traction motor. The rotor is transferred to the stator. According to the mathematical model of rail transit traction motor calculation in Fig. 1, the power factor ($\cos \varphi_2$) on the rotor side of the traction motor can be derived, such as (6):

$$\cos \varphi_2 = \frac{\frac{R_2}{S}}{\sqrt{\left(\frac{R_2}{S}\right)^2 + (L_2)^2}} \quad (6)$$

The electromagnetic torque (T_{em}) calculation formula of the traction motor is shown in (7). In (7), C_{T1} is the traction motor torque constant, and the electromagnetic torque (T_{em}) is less than $0(T_{em})$. It shows that the traction motor is in the braking mode.

$$T_{em} = C_{T1} \varnothing_m \dot{I}_2 \cos \varphi_2 \quad (7)$$

When the rail transit traction motor is operating under braking conditions, the value range of the power factor angle (φ_1) on the stator side of the traction motor is ($90^\circ, 180^\circ$). According to the mathematical model of the rail transit traction motor calculation in Fig. 1, the calculation formulas for the active power P_1 and the reactive power Q_1 on the stator side of the traction motor can be derived, as shown in (8) and (9):

$$P_1 = m_1 \dot{U}_s \dot{I}_1 \cos \varphi_1 \quad (8)$$

$$Q_1 = m_1 \dot{U}_s \dot{I}_1 \sin \varphi_1 \quad (9)$$

When the rail transit traction motor is operating under braking conditions, the rail transit traction motor will be in a state of generating operation, its stator side active power will be fed back to the grid, and its reactive power still needs to be absorbed from the grid side [3].

3. Analysis of Traction Characteristics of Traction Motors in Rail Transit

When the rail transit traction motor starts, it needs to ensure that its armature current is constant. It can achieve the goal of speed regulation by changing its terminal voltage, and the traction frequency converter realises the control by adopting the control mode of constant voltage–frequency ratio. Thereby, the calculation formula of the main magnetic flux (\varnothing_m) is obtained (\varnothing_m), as shown in (10). In (10), $k_{\omega 1}$ represents the fundamental winding coefficient of the stator, N_1 is the number of series turns of each phase winding of the rail transit traction motor stator [3], [11].

$$\varnothing_m = \frac{\dot{E}}{-j4.44k_{\omega 1}N_1f_1} \propto \frac{\dot{E}}{f_1} \approx \frac{\dot{U}_s}{f_1} \quad (10)$$

When the rail transit traction motor is in the constant flux area, the calculation (11) of the electromagnetic torque

(T_{em}) of the traction motor can be derived from (3) and (4). In (11), Ω_1 is the synchronous angular velocity of the traction motor (rad/s); and p is the number of pole pairs of the traction motor.

$$T_{em} = \frac{P_{em}}{\Omega_1} = \frac{3pf}{2\pi} \left(\frac{\dot{E}}{f} \right)^2 \frac{1}{\frac{R_2}{S} + \frac{SL_2^2}{R_2}} \quad (11)$$

Differentiate (11) and make it equal to zero. Then the maximum electromagnetic torque (T_m) of the traction motor can be obtained, as shown in (12). In (12), L'_2 is the equivalent value of the rotor leakage reactance coefficient, which is expressed as (13):

$$T_m = \frac{1}{2} \frac{3p}{2\pi} \left(\frac{\dot{E}}{f_1} \right)^2 \frac{1}{2\pi L'_2} \propto \left(\frac{\dot{E}}{f_1} \right)^2 \quad (12)$$

$$L'_2 = \frac{L_2}{2\pi f_1} \quad (13)$$

When the rail transit traction motor is operating in the constant flux working area, the maximum electromagnetic torque (T_m) of the rail transit traction motor can also be considered as a constant value. The calculation (14) of the mechanical power (P) of the traction motor can be derived from the (11), and Ω is the mechanical angular speed of the rail transit traction motor (rad/s).

$$P = \Omega T_{em} \quad (14)$$

When the rail transit traction motor is operating in the constant flux working area, its output power will increase with the increase of the traction motor speed.

When the rail transit traction motor works at the speed of the rated frequency point, the traction frequency converter slowly raises the armature voltage to the maximum allowable voltage value. When the speed of the traction motor is increased from the fundamental frequency, the calculation (15) for the maximum torque (T_M) of the traction motor and the frequency (f_1) of the traction inverter (that is, the stator side frequency of the traction motor) can be obtained by (11). In (15), U_1 is a constant armature voltage value.

$$T_M = \frac{3}{4} \frac{pU_1^2}{\pi^2 (L_1 + L_2) f_1^2} \propto \frac{1}{f_1^2} \quad (15)$$

As the stator side frequency (f_1) of the rail transit traction motor increases, the electromagnetic torque of the traction motor decreases and the speed increases. From (14), the output mechanical power of the rail transit traction motor is basically constant; but from (10), it can be seen that when the frequency is above the fundamental frequency, the armature voltage of the traction inverter remains unchanged, and the air gap flux decreases as the speed of the traction motor increases. Therefore, when the traction motor works above the fundamental frequency, it will work in the field weakening and constant power speed control working area.

With the continuous increase in the speed of rail transit traction motors, if the terminal voltage of the motor remains unchanged, the value of its excitation current will continue to decrease. Within this range, the power

of the rail transit traction motor will no longer remain unchanged and will decrease as the speed of the traction motor increases. At the same time, the traction power calculation formula $P = CFv = U_a I_a$ can be obtained, and C is the transmission efficiency constant of the traction motor, F is the traction around the wheel (kN), v is the operating speed of rail transit vehicles (km/h); U_a , I_a are the armature voltage and armature current of the traction motor [3], [12].

With the continuous increase in the speed of rail transit traction motors, its output power will inevitably decrease, and its armature current and traction force will gradually decrease accordingly, so rail transit traction motors are in the natural characteristic area [3], [16].

4. Analysis of Braking Characteristics of Traction Motors in Rail Transit

If the rail transit traction motor is in the braking mode, the traction motor is in the power generation operation state. When the rail transit traction motor is in the state of high-speed braking, its back electromotive force will be relatively large, and because the braking resistor (R_z) is directly connected to the two ends of the armature during braking. The braking current calculation (16) can be obtained according to Fig. 1. In (16), C_e is the potential constant of the traction motor.

$$i_z = \frac{\dot{E}}{R_z} = \frac{\varnothing_m C_e}{R_z} \quad (16)$$

The solution and selection of braking resistance (R_z) can be calculated and solved according to (17). In (17), P is the braking power of the traction motor; U_d is the DC side voltage of the traction inverter; and K is the braking margin coefficient, it usually can be taken as a fixed value of 1.3 [13].

$$R_z \leq \frac{(U_d K_1 K_2)^2}{PK} \quad (17)$$

It can be obtained from the calculation (16) of the braking current. In order to ensure the i_z (brake current) of the rail transit traction motor, if its speed is reduced, its excitation current needs to be increased accordingly. At the same time, its braking power will inevitably increase accordingly, so it works in the magnetisation control area. If the rail transit traction motor works at the critical point of the two working areas of magnetisation and voltage regulation, its excitation current and braking current (i_z) have reached the maximum allowable value, and its speed is the mode of magnetisation control. The speed of the traction motor is the minimum allowable value required by the modulated magnetic control mode.

If the traction motor takes the maximum value of excitation current, the value of its excitation current has reached a state that cannot be changed, and as its speed continues to decrease, i_z and P will also decrease. Based on this, the calculation (18) of the terminal voltage (U) of the traction motor can be obtained. In (18), K_s is the excitation coefficient, U is the terminal voltage of the traction motor, I_a is the armature current, n_1 is the

Table 1
Performance Parameter Table of the Tested Traction Motor

Num	Performance Parameter Name	Performance Parameter Index
1	Phase	3
2	Number of pole pairs	4
3	Power (continuous rating)/kW	200
4	Frequency (continuous rating)/Hz	80
5	Voltage (continuous rating)/V	1170
6	Current (continuous rating)/A	125
7	Maximum operating speed (wear wheel diameter)/r/min	3889
8	Maximum design speed (wear wheel diameter)/r/min	4375

speed of the traction motor, C_e is the potential constant of the traction motor, and R is the total resistance of the armature circuit [3], [14].

$$U = (K_s C_e n_1 + R) I_a \quad (18)$$

According to the calculation (18) of the terminal voltage (U) of the traction motor, the terminal voltage has a linear relationship with the speed (n_1) and armature current (I_a), then the traction motor is in the working area of voltage regulation control.

5. Traction Braking Characteristic Test of Rail Transit Traction Motor

5.1 Rail Transit Traction Motor Test Platform and Principle

The test object of this article is the 200 kW Bombardier MJC250-7 rail transit traction motor used in Lanzhou Rail Transit Co., Ltd. Its main performance parameters are shown in Table 1.

Based on the previous analysis of the traction braking characteristics of rail transit traction motors, the rail transit traction motor intelligent comprehensive test system produced by Hunan Xinen Intelligent Technology Co., Ltd. (as shown in Figure. 2) was used to test the traction characteristics. The traction braking characteristics of the 200 kW Bombardier MJC250-7 rail transit traction motor used in Lanzhou Rail Transit Co., Ltd. were tested. In this rail transit traction motor intelligent comprehensive test system, the temperature sensor (PT100), temperature inspection instrument (CK-XME), power analyser (WT1800), DC resistance measuring instrument (Amber

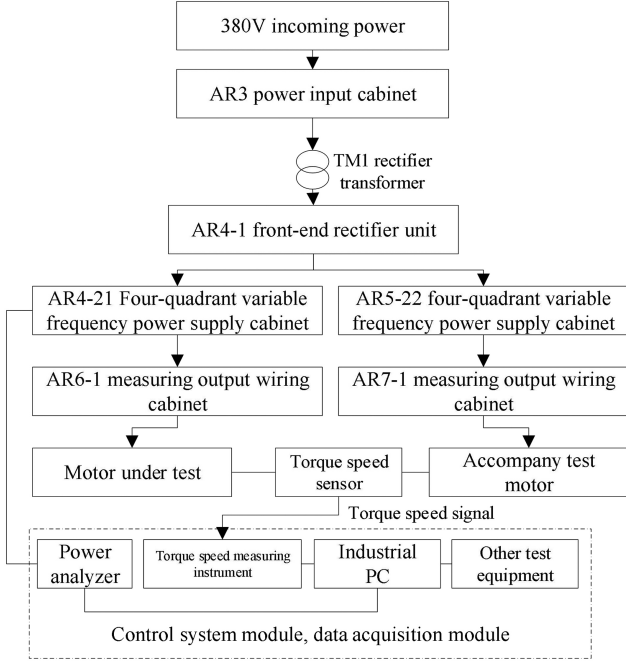


Figure 2. Block diagram of the intelligent comprehensive test system for rail transit traction motors.

AT516/AT516L), AC withstand voltage/insulation measuring instrument (TH9310B), and other instruments are used. The characteristic parameters, such as current, voltage, and power factor of rail transit traction motors, are tested, calculated, and displayed.

The intelligent comprehensive test system of rail transit traction motor adopts the method of towing load to realise the test of traction braking characteristics. The accompanying test motor constructs a pair of towing units through a coupling and the tested motor. The energy is fed back to the AC bus through the AR4-21 and AR5-22 four-quadrant variable frequency power cabinets for recycling. When testing the traction characteristics, the tested traction motor works as a traction motor and works in an electric state. At each test frequency point, the host computer (industrial computer: Advantech IPC-610MB-30LDE) passed the test of the measured motor armature voltage and other related parameters. The closed-loop control of the output frequency and voltage of the AR4-21 four-quadrant variable frequency power supply cabinet is realised. Finally, with the help of the frequency difference between the AR4-21 and AR5-22 four-quadrant variable frequency power supply cabinets, the traction power control of the tested motor (the tested traction motor) is realised. When testing, the braking characteristics and the traction characteristics of the test method adopted are roughly the same, the difference is that when the braking characteristics test, the rail transit traction motor uses the “regenerative braking” method to be in the power generation state [3], [15].

5.2 Traction Braking Characteristic Test Method

The test method of the traction characteristics at the 61 Hz frequency point is as follows: It uses the control mode

of constant voltage–frequency ratio ($\frac{U_s}{f_1} = \text{constant}$) to start the AR4-21 four-quadrant variable frequency power supply cabinet. After the motor under test (the traction motor under test) rotates, then the output frequency of the traction frequency converter (AR4-21 four-quadrant frequency conversion power supply cabinet) is given to 61 Hz. When the frequency of the motor under test (the traction motor under test) reaches 61 Hz, the feedback inverter (AR5-22 four-quadrant variable frequency power supply cabinet) is started in a constant frequency transformation method at 61 Hz/0V, and then the terminal voltage of the generator gives the rated voltage. Then the output frequency of the traction frequency converter (AR4-21 four-quadrant frequency conversion power supply cabinet) is adjusted in a small range, and according to the shaft power data measured by the intelligent comprehensive test system of the rail transit traction motor, the motor under test (the traction motor under test) is finally selected. The traction power is given to 270 kW, and the relevant characteristic parameters of the tested motor (the tested traction motor) are obtained [3]. In the same way, the traction characteristic test method of the remaining frequency points is the same as the 61 Hz frequency point test method.

The test method of the braking characteristics at the 101 Hz frequency point is as follows: Start the AR5-22 four-quadrant variable frequency power cabinet using the control mode of constant voltage–frequency ratio ($\frac{U_s}{f_1} = \text{constant}$). After the test motor rotates, the output frequency of the drag inverter (AR5-22 four-quadrant variable frequency power supply cabinet) is adjusted to 101 Hz. When the traction inverter (AR5-22 four-quadrant frequency conversion power supply cabinet) reaches 101 Hz, the traction inverter (AR4-21 four-quadrant frequency conversion power supply cabinet) will be started at 101 Hz/0V in a constant frequency transformation method, and the traction motor (AR4-21 four-quadrant variable frequency power supply cabinet) terminal voltage reaches to the rated voltage. Then the output frequency of the traction frequency converter (AR4-21 four-quadrant frequency conversion power supply cabinet) is adjusted, and the shaft power data measured by the torque/speed sensor. Adjust the braking power of the motor under test (the traction motor under test) to 468 kW, and the relevant characteristic parameters of the motor under test are obtained [3]. In the same way, the traction characteristic test method of the remaining frequency points is the same as the 101 Hz frequency point test method.

5.3 Rail Transit Traction Motor Test Results

The test data (shown in Table 2) and characteristic test curves (shown in Fig. 3) of the traction characteristics of rail transit traction motors are obtained through the test of the intelligent comprehensive test system for rail transit traction motors. Analysis of the test results shows the MJC250-7 traction motor works in the constant torque area within the frequency range of (0 Hz, 61 Hz), and its torque remains unchanged at 1418 N·m. At the same time,

Table 2
Traction Characteristic Parameter Table of the Tested Traction Motor

Num	Speed/r/min	Frequency/Hz	Voltage/V	Current/A	Output Power/kW	Slip/Hz	Efficient	Torque/N·m
1	228	8.4	181.7	204.2	33.8	0.87	0.652	1418
2	455	16	319.3	204.5	67.5	0.88	0.767	1418
3	1362	46.2	871.9	205.5	202.2	0.89	0.886	1418
4	1589	53.8	1010.3	205.8	235.9	0.89	0.897	1418
5	1816	61	1148.7	205.9	269.6	0.89	0.907	1418
6	2043	69	1170	178.8	269.9	0.93	0.916	1263
7	2269	76.6	1170	166.8	270.3	1.02	0.921	1138
8	2496	84.3	1170	163.5	270.5	1.13	0.921	1036
9	2723	92	1170	163.5	270.9	1.25	0.919	951
10	2814	95	1170	160	265.5	1.27	0.918	902
11	2949	99.6	1170	152.9	253.9	1.27	0.918	823
12	3177	107.1	1170	142.6	236.6	1.27	0.917	712
13	3404	114.7	1170	133.8	221.4	1.27	0.914	622
14	3631	122.3	1170	126.5	208.4	1.28	0.911	549
15	3889	131	1170	128.9	210.2	1.42	0.904	517

its traction power increases with the increase in speed. The output power of MJC250-7 traction motor is about 270 kW at 61 Hz; The MJC250-7 traction motor works in the constant power range in the frequency range (61 Hz, 92 Hz), and its output power remains unchanged at 270 kW; the torque of the MJC250-7 traction motor decreases as the speed increases. At 92 Hz frequency point, its torque value is 1418 N·m; When the MJC250-7 traction motor is in the frequency range of (92 Hz, 131 Hz), the traction motor runs in the natural characteristic area, and its output power and torque decrease with the increase of the motor speed.

Figure 3 shows the traction characteristic test curve of the MJC250-7 traction motor. The following conclusions can be drawn by comparing and analysing its ideal traction characteristic curve: The constant torque region of the ideal traction characteristic curve and the traction characteristic test curve are both in the range of (0 Hz, 61 Hz), the constant power region is in the range of (61 Hz, 92 Hz), and the natural characteristic region is in the range of (92 Hz, 131 Hz). The boundary of the working area in the traction characteristic test curve of the MJC250-7 traction motor is basically the same as the ideal traction characteristic curve. When the MJC250-7 traction motor is in the constant torque area, the torque test data is 1418 N·m, which is roughly the same as the torque value of 1445 N·m in the ideal traction characteristic curve. When the MJC250-7 traction motor is in the constant power zone, the output power test data is 270 kW, which is roughly the same as the power value of 270 kW in the ideal traction characteristic curve.

The test data (shown in Table 3) and characteristic test curves (shown in Figure. 4) of the braking

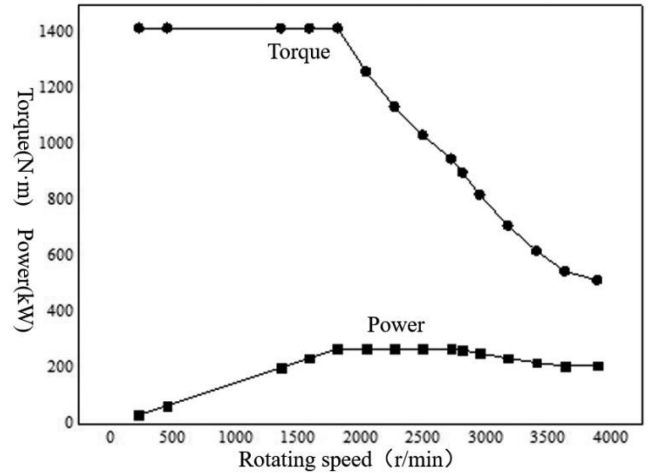


Figure 3. Traction motor traction characteristic test curve.

characteristics of the MJC250-7 rail transit traction motor are obtained through the test of the intelligent comprehensive test system for rail transit traction motors. Analysis of the test results shows: The MJC250-7 traction motor runs in the frequency range (109.5 Hz, 127.3 Hz) in the field of magnetic modulation control. In this frequency range, the braking current of the MJC250-7 traction motor increases with the speed of the MJC250-7 traction motor. Increase and slightly increase, the traction motor torque decreases with the increase of the MJC250-7 traction motor speed, and the output power remains basically unchanged; When the MJC250-7 traction motor works at 109 Hz, the braking current of the traction motor is as high as 225.5A,

Table 3
Braking Characteristic Parameter Table of Tested Traction Motor

Num	Speed/r/min	Frequency/Hz	Voltage/V	Current/A	Output Power/kW	Slip/HZ	Efficient	Torque/N·m
1	0	—	—	—	—	—	—	1445
2	447	14	232	204.4	67.6	0.86	0.716	1445
3	669	21.4	368.8	204.2	101.3	0.87	0.795	1445
4	892	28.8	505	203.9	135.2	0.87	0.833	1445
5	1115	36.3	641.2	203.6	168.9	0.87	0.857	1445
6	1338	43.7	777.5	203.4	202.7	0.87	0.874	1445
7	1561	51.1	913.8	203.4	236.4	0.87	0.888	1445
8	1784	58.6	1050.1	202.8	270.2	0.87	0.898	1445
9	2006	66	1186.4	202.6	303.9	0.86	0.905	1445
10	2229	73.4	1286	197.9	337.7	0.92	0.909	1445
11	2452	80.6	1286	190.7	371.5	1.07	0.916	1445
12	2675	87.9	1286	197.7	405.2	1.26	0.918	1445
13	2898	95.1	1286	210.8	438.9	1.48	0.914	1445
14	3096	101.4	1286	225.4	468.9	1.74	0.908	1445
15	3118	102.2	1286	225.4	468.8	1.75	0.907	1435
16	3343	109.5	1286	225.7	468.4	1.92	0.903	1339
17	3377	110.6	1286	225.8	468.5	1.93	0.903	1326
18	3404	111.5	1286	225.8	468.4	1.95	0.902	1315
19	3647	119.4	1286	226.9	467.8	2.14	0.897	1226
20	3889	127.3	1286	228.9	467.3	2.34	0.889	1148

the output power reaches 468.3 kW, and the traction motor torque is 1338N·m; When the MJC250-7 traction motor is in the frequency range (0 Hz, 109.5 Hz), the MJC250-7 traction motor runs in the voltage regulation control work area, and its torque remains unchanged at 1445 N·m; When the MJC250-7 traction motor is in the frequency range of (0 Hz, 101.4 Hz), the output power increases with the increase of the speed of the traction motor, but when the frequency increases to the range of (101.4 Hz, 109.5 Hz), The output power remains basically unchanged; the terminal voltage of the MJC250-7 traction motor increases with the increase of the traction motor speed in the frequency range (0 Hz, 66 Hz), and the terminal voltage in the frequency range (73.4 Hz, 109.5 Hz) stable at 1286 V unchanged. Traction characteristic curves are drawn based on test data, as shown in Table 2 and Fig. 3. Compared with the traction characteristic curve of the motor itself, the measured results of the test system are basically consistent with the qualified motor parameters.

Figure 4 shows the braking characteristic test curve of the MJC250-7 traction motor, and the following conclusions can be drawn by comparing and analyzing its ideal braking characteristic curve: Both the ideal traction characteristic curve and the traction characteristic test

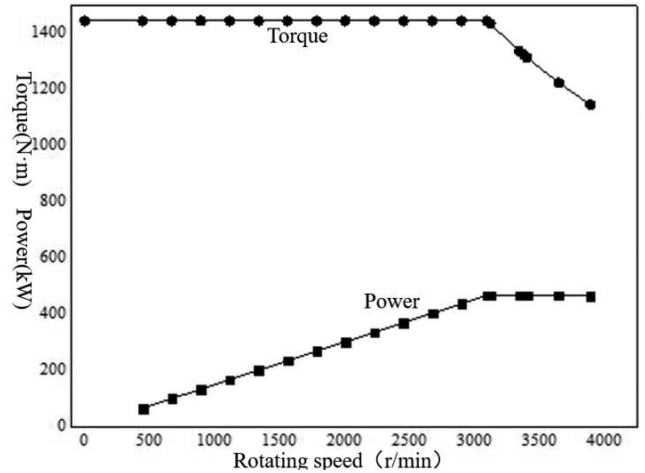


Figure 4. Test curve diagram of braking characteristic of traction motor.

curve's magnetic modulation control work area are within the frequency range of (109 Hz, 127 Hz), and the voltage regulation control work area is within the frequency range of (0 Hz, 109 Hz). Therefore, MJC250-7 traction

motor, the demarcation point of the braking characteristic test curve and the working area of its ideal braking characteristic curve remains basically the same. When the MJC250-7 traction motor is working in the voltage regulation control area, the torque data obtained by the test remains unchanged at 1445 N·m, which is the same as the median value of the ideal braking characteristic curve of the MJC250-7 traction motor.

Traction braking characteristic curves are drawn based on test data, as shown in Table 3 and Fig. 4. Compared with the traction braking characteristic curve of the motor itself, the measured results of the test system are basically consistent with the qualified motor parameters.

6. Conclusion

- (1) In the process of testing the traction braking characteristics of the rail transit traction motor, when the rail transit traction motor starts or stops, the control strategy of constant voltage–frequency ratio is adopted, and it is necessary to ensure that the value of $\frac{\dot{U}_s}{f_1}$ cannot be too large. According to (10), if the armature voltage increases or decreases rapidly with the frequency of the stator side, the air gap flux (\varnothing_m) is very likely to exceed its allowable range. As a result, its excitation current rises sharply, which ultimately affects its mechanical and electrical characteristics. Therefore, when the rail transit traction motor is started and stopped, it should be ensured that the value of $\frac{\dot{U}_s}{f_1}$ cannot be too large, and the two methods provided in document [3] can be adopted to ensure the start and stop of the rail transit traction motor. The first method is to appropriately increase its starting voltage \dot{U}_s , which can compensate the stator voltage drop, then the increase speed of E (main flux induced electromotive force) is slowing down; The second method is to keep \dot{U}_s unchanged. First, the constant voltage–frequency ratio control mode is used to gradually establish the magnetic field of the traction motor, so that when it starts to reach the rated frequency, its armature voltage is slightly less than its rated voltage. Then, the rated frequency is maintained at a constant value through the control mode of constant frequency transformation, and finally the purpose of the armature voltage is gradually increased, and it is increased to the rated voltage. Through the second method, the increase rate of $\frac{\dot{U}_s}{f_1}$ of the rail transit traction motor can be significantly reduced at the same time [3].
- (2) In the process of testing the braking characteristics of rail transit traction motors, because at the 109 Hz frequency test point, the output power of the 200 kW MJC250-7 traction motor is required to reach 468 kW, so it needs to increase the frequency difference of the traction unit by AR4-21 and AR5-22, but it will cause the current to be much larger than its rated current, and ultimately lead to changes in the mechanical and electrical characteristics of the traction motor, making the output power unable to meet the purpose of its braking test. Therefore, by appropriately increasing its

terminal voltage, and making it higher than the rated value of the armature voltage, the goal of restraining the braking current of the traction motor is finally achieved. According to $P = CFv = U_a I_a$: In the case of the same braking current of the traction motor, if the terminal voltage is appropriately increased, the braking power will be significantly increased to meet the power requirements of the braking characteristic test.

- (3) Theoretical level: Using the general mathematical model of rail transit traction motor, the traction braking characteristics of rail transit traction motor are analysed in detail, and the control strategy of rail transit traction motor operation and the typical characteristic parameters of rail transit traction motor are deduced. Practical level: The traction braking characteristic test of the MJC250-7 rail transit traction motor has been completed, which provides a reference experience for rail transit operators to carry out the traction braking characteristic test of the traction motor.

Acknowledgement

This work was supported by Hunan Provincial Natural Science Foundation of China (NO:2020JJ6095), Scientific Research Project of Hunan Provincial Department of Education (NO: 21B0896) and (NO: 20B392).

References

- [1] J. Wenzheng, H. Xuefei, X. Zhenxing, and L. Yue, State of the art and trend of intelligent maintenance of urban rail transit facilities and equipment in China, *Urban Rapid Rail Transit*, 33(2), 2021, 14–19.
- [2] Z. Linde and G. Hongzhen, Simulation research on new type asynchronous traction motor test system, *Energy-Saving Technology*, 22(127), 2004, 28–29.
- [3] H. Bo-Jun, J. Hua-Bing, X. Quan-Hua, L. Wen-Chao, and L. Jin-Cheng, Test method of traction and braking characteristics for a novel urban-rail traction motor, *Electric Drive for Locomotives*, (5), 2012, 70–75.
- [4] T. Caixia, Y. Yanping, and L. Xiao, Simulation research on traction characteristics of metro traction motor, *Automation and Instrumentation*, (6), 2012, 25–27.
- [5] W. Renqing, Metro vehicle braking characteristics and optimal analysis of electro-pneumatic conversion parameters, *Urban Rail Transit Research*, 22(12), 2019, 92–95.
- [6] G. Qidong, *Traction calculation and operation energy consumption analysis of subway trains*. (Shenzhen: Shenzhen University, 2019).
- [7] L. Wei, C. Wenguang, C. Chaolu, and X. Peijin, Traction and electric braking characteristic design and performance calculation simulation of Chongqing metro line 6 vehicles, *Electric Drive for Locomotives*, (3), 2012, 52–54+61.
- [8] H. Hao, C. Xiao, and H. Wei, Method of calculating vehicle traction/brake envelope by using binary search and Lagrangian interpolation algorithm, *Electric Drive for Locomotives*, (5), 2012, 99–102+106.
- [9] L. Yifeng, G. Peiqing, and G. Xifeng, Calculation of the characteristic curve of asynchronous traction motor powered by inverter, *Electric Drive for Locomotives*, (6), 1997, 8–11.
- [10] M. Ehsani, Y. Gao, and S. Gay, Characterization of electric motordrives for traction applications, *Industrial Electronics Society*, (1), 2003, 891–896.
- [11] W. Asaki and F. Noriko, Traction performance of high-speed train rolling stock, *China Railway Science*, 25(4), 2004, 32–36.

- [12] D. Rongjun, The matching of AC drive locomotive traction characteristic curve and converter-traction motor system, *Electric Drive for Locomotives*, (6), 1999, 14–16.
- [13] W. Yuhua, M. Jianlin, and W. Yuanfang, The research of traction motor energy-saving regenerative braking control technology, *Proc. Int. Conf. on Intelligent Computation Technology and Automation*, Changsha, 2010, 930–933.
- [14] S. Wen, G. Jun, T. Laisheng, and W. Guangnin, Study on effect of voltage distortion on insulation of variable-frequency adjustable-speed traction motor, *Proc. Annual Report Conf. on Electrical Insulation and Dielectric Phenomena*, Nashville, TN, 2005, 249–252.
- [15] Z. Yunfeng and L. Huaizhen, Design of performance test bench for small power permanent magnet synchronous motor, *Micromotors*, 52(8), 2019, 99–102.
- [16] G. Sizhou, Z. Yihuang, Y. Haiyan, and W. Jian, Research on control strategies for suppressing the starting peak current of asynchronous traction motors, *Electric Drive for Locomotives*, (5), 2008, 23–26+29.
- [17] S. Ghosh, H. Goud, P. Swarnkar, and D.M. Deshpande, Design of an optimized adaptive PID controller for induction motor drive, *Mechatronic Systems and Control*, 49(3), 2021, 164–170.
- [18] V. Shirish Murty, S. Jain, and A. Ojha, Suitability of linear switched reluctance motor for advanced electric traction system, *Mechatronic Systems and Control*, 49(3), 2021, 142–148.
- [19] X. Shi, X. Zhu, and J. Zhang, Simulation and experimental analysis of drive motor stator current under local fault of gear, *Mechatronic Systems and Control*, 49(2), 2021, 74–82.
- [20] G. Kevin, G. Steven, B. Karthik, E. Refaie, and M.E.-R. Ayman, Design and testing of a carbon-fiber-wrapped synchronous reluctance traction motor, *IEEE Transactions on Industry Applications*, 54(5), 2018, 4207–4217.
- [21] S. Paul, P.-W. Han, J. Chang, Y.-D. Chun, and J.-G. Lee, State-of-the-art review of railway traction motors for distributed traction considering South Korean high-speed railway, *Green Energy and Intelligent Transportation*, 8(11), 2022, 14623–14642.
- [22] K. Keerti, A. Nataraj, and M. Prabhakar, Design, development and testing of traction motor speed sensor used in Indian railway locomotive, *International Journal of Computer Applications*, 182(8), 2018, 9–12.



Jun Yan received the B.Sc. degree in electrical control from Wuhan University of Science and Technology, China. Now, he is a Professor with Hunan Railway Professional Technical College. His research field of centers on electrical control.



Li Yang received the M.Sc. degree in signal and information processing from ShenZhen University, China. She is an Associate Professor with Hunan Railway Professional Technical College. Her research field of centers on electric automation.



Hui Zhang received the B.Sc. degree in communication engineering from Lanzhou Jiaotong University, China. He is the Deputy General Manager of the operation branch of Lanzhou Rail Transit Co., Ltd. His research field of centers on electrical control.

Biographies



Yong Chao Xie received the M.Sc. degree in communication and information system from Southwest Jiaotong University, China. He is a Professor with Hunan Railway Professional Technical College. His research field of centers on motor control.



Canhui Wu is the General Manager of Hunan Xinen Intelligent Technology Co., Ltd. He is committed to the research of intelligent measurement and control solutions for the motor, RV and new energy industries.